Purification of Single-Walled Carbon Nanotubes by a Highly Efficient and Nondestructive Approach

Jie Ma and Jian Nong Wang*

School of Materials Science and Engineering, Shanghai Jiao Tong University, 800 Dong Chuan Road, Shanghai 200240, P. R. of China

Received October 18, 2007

Single-walled carbon-nanotubes (SWCNTs) in their as-grown state contain a large quantity of impurities such as catalytic particles and encapsulating graphitic shells. Previous purification approaches usually depended upon severe oxidation. But such oxidation in either a gas phase or a liquid phase induces structural destruction and a big loss of the SWCNT material. In this study, a new method is reported that involves transformation of catalytic iron particles to iron oxide at a low temperature of 400 °C, removal of graphitic shells by reaction with the encapsulated iron oxide at a high temperature of 800–900 °C, and final elimination of iron oxide particles by HCl. Experimental results, based on transmission electron microscopy, Raman spectroscopy, thermogravimetric analysis, and near-infrared spectroscopy, show that catalytic particles and encapsulating graphitic shells can be removed. More importantly, this highly efficient purification induces little damage to the graphitic structure of SWCNTs. These observations are in strong contrast with those from the samples purified in HCl or HNO_3. The present method may be applied for highly efficient and nondestructive purification of CNT materials of any origin to be used in wide areas.

1. Introduction

Single-walled carbon nanotubes (SWCNTs) were first synthesized in 1993 by Iijima et al.[1] and Bethune et al.[2] using the sublimation of graphite by electric arc discharge in the presence of a metallic catalyst. SWCNTs have attracted a great deal of attention due to their unique physical, chemical, and mechanical properties.[3,4] They are expected to be useful in many different applications, such as field emission displays, supercapacitors, batteries, hydrogen storage, nanotechnology tools, chemical sensors, electronic devices, and polymeric composites.[5–7]

In order to obtain the optimal performance of SWCNTs in various applications, high purity is a criterion. However, initial SWCNTs synthesized by electric arc-discharge,[8] laser vaporization,[9] and chemical vapor deposition methods[10,11] often contain a large quantity of impurities, including small catalytic metal particles and carbonaceous byproduct such as fullerenes, amorphous or graphitic carbon particles, and multiwalled carbon nanotubes (CNTs). While these carbonaceous byproduct can be minimized by optimizing experimental conditions, the catalytic metal particles are always present, as they are essential to the growth of SWCNTs. The current methods for purification can be categorized into three major classes: physical separation, gas-phase oxidation, and liquid-phase oxidation. The physical-separation method includes procedures of dispersion of SWCNTs in a surfactant solution and then separation of SWCNTs by filtration,[12] centrifugation,[13] or a chromatographic technique.[14] Highly pure and length-selected SWCNTs in aqueous solutions can be obtained by column chromatography. However, this method is only useful for the preparation of a very small amount of purified samples but not for large-scale applications. The gas-phase oxidation under air, oxygen, ozone, H_2S and CO_2 atmospheres at high temperature have been used to selectively eliminate the unwanted amorphous carbon materials.[15] However, the oxidation temperature and time could not be easily controlled, owing to the close similarity of the chemical properties of the CNTs with the remaining carbonaceous materials. Alternatively, liquid-phase oxidation was reported, with strong oxidative agents such as HNO_3, $HClO_4$, and $KMnO_4/H_2SO_4$, but it has been shown that such acid treatments led to partial destruction of the nanotube

* Fax: +86-21-54743174. E-mail: jnwang@mail.sjtu.edu.cn.

(1) Iijima, S. *Nature* **1991**, *354*, 56–58.
(2) Bethune, D. S.; Kiang, C. H.; De Vries, M. S.; Gorman, G.; Savoy, R.; Vazquez, J.; Beyers, R. *Nature* **1993**, *363*, 603–605.
(3) Snow, E. S.; Perkins, F. K.; Houser, E. J.; Badescu, S. C.; Reinecke, T. L. *Science* **2005**, *307*, 1942–1945.
(4) Zhang, M.; Atkinson, K. R.; Baughman, R. H. *Science* **2004**, *19*, 1349–1358.
(5) Guo, A.; Fu, Y.; Wang, C.; Guan, L.; Liu, J.; Shi, Z.; Gu, Z.; Zhang, X. *Nanotechnology* **2007**, *18*, 125206–125210.
(6) Haggenmueller, R.; Gommans, H. H.; Rinzler, A. G.; Fischer, J. E.; Winey, K. I. *Chem. Phys. Lett.* **2000**, *330*, 219–225.
(7) Zhang, T.; Mubeen, S.; Bekyarova, E.; Yoo, B. Y.; Haddon, R. C.; Myung, N. V.; Deshusses, M. A *Nanotechnology.* **2007**, *18*, 165504–165509.
(8) Yao, M.; Liu, B.; Zou, Y.; Wang, L.; Li, D.; Cui, T.; Zou, G.; Sundqvist, B. *Carbon* **2005**, *43*, 2894–2895.
(9) Blackburn, J. L.; Yan, Y.; Engtrakul, C.; Parilla, P. A.; Jones, K.; Gennett, T.; Dillon, A. C.; Heben, M *Chem. Mater.* **2006**, *18*, 2558–2566.
(10) Song, L. C.; Sun, L.; Jin, C.; Liu, L.; Ma, W.; Liu, D.; Xie, S *Adv. Mater.* **2006**, *18*, 1817–1820.
(11) Hata, K.; Futaba, D. N.; Mizuno, K.; Namai, T.; Yumura, M.; Iijima, S. *Science* **2004**, *306*, 1362–1364.
(12) Montoro, L. A.; Luengo, C. A.; Rosolen, J. M.; Cazzanelli, E.; Mariotto, G. *Diamond Relat. Mater.* **2003**, *12*, 846–849.
(13) Duesberg, S.; Muster, J.; Byrne, H. J.; Roth, S.; Burghard, M. *Appl. Phys. A: Mater. Sci. Process.* **1999**, *69*, 269–274.
(14) Holzinger, M.; Hirsch, A.; Bernier, P.; Duesberg, G. S.; Burghard, M. *Appl. Phys. A: Mater. Sci. Process.* **2000**, *70*, 599–602.
(15) Zimmerman, J. L.; Bradley, R. K.; Huffman, C. B.; Hauge, R. H.; Margrave, J. L. *Chem. Mater.* **2000**, *12*, 1361–1366.

10.1021/cm8001699 CCC: $40.75
Published on Web 03/25/2008

Table 1. Different Purification Processes

process	air oxidation (400 °C, 45 min)	high-temperature treatment (800 °C/ 900 °C, 60 min)	HCl reflux (100 °C, 4 h)	HNO_3 reflux (100 °C, 4 h)	air oxidation (400 °C, 45 min)
1	yes		yes		
2	yes			yes	
3	yes	yes	yes		
4	yes	yes	yes		yes

sample with the walls of the SWCNTs being damaged, distorted, or even segmented.[16] Furthermore, the "purified" SWCNT bundles could be covered by debris from oxidation.[17]

The main problem with previous methods is that the metal particles that play a catalytic role on CNT growth are encapsulated by graphitic carbon cages or shells. The graphitic structure presents high resistance to oxidation or acid treatment, and thus carbon cages and the enclosed metal particles usually remain after purification. In order to achieve a sufficient purification, severe oxidation has to be imposed. But in this case, there is an inevitable big loss of and damage to the CNTs. Therefore, to date, it is still a great challenge to seek a method that can purify SWCNTs efficiently but keep the graphitic structure of the tubes intact.

In this paper, we report a simple and efficient method for purifying SWCNT raw materials. Our work focuses on the removal of the graphitic carbon cages and enclosed metal particles with little destruction to the CNT structure. This is done by transformation of the metallic particles at a low temperature to iron oxide and then removal of the graphitic cages by reaction with the enclosed metal oxides at a high temperature. With a final treatment in the mild acid of HCl, the original catalytic particles with graphitic cages could be eliminated.

2. Experimental Section

The initial SWCNTs were prepared by spray pyrolysis, in which ethanol was used as a carbon feedstock, ferrocene as a catalyst, and thiophene as a growth promoter. One gram of ferrocene and 1 mL of thiophene were dissolved in 100 mL of ethanol to prepare the solution for spray. A quartz tube of 3 cm in diameter and 1 m in length was heated up to 1150 °C using a tubular furnace with a heating length of 70 cm. In raising the temperature, Ar flow was initiated in the quartz tube in order to purge air from the reaction chamber. The ethanol solution dissolved with ferrocene and thiophene was supplied by an electronic squirming pump at the rate of 0.4 mL min^{-1} and sprayed through a nozzle with the Ar flow at a rate 160 L h^{-1}. After several hours of pyrolysis, the supply of ethanol was terminated, and the sample was collected from a glass bottle connected to the quartz tube.

In order to remove the impurities contained in the pristine sample (CNT-0), such sample was treated by four different processes for the purpose of comparison (Table 1). All processes started with an air-oxidation step. To do this, the pristine sample in a quartz boat was put in a quartz tube and heated in air at 400 °C for 45 min to oxidize Fe nanoparticles. Air was introduced into the quartz tube at a slow rate to provide oxygen continuously. After air oxidation, the sample was treated by different processes.

In process 1, the sample was directly refluxed in 12 M HCl at 100 °C for 4 h (CNT-1). In process 2, the sample was directly refluxed in 14 M HNO_3 at 100 °C for 4 h (CNT-2). In process 3, however, the sample was further heat-treated at 800 or 900 °C for 60 min under the protection of Ar gas and then refluxed in 12 M HCl at 100 °C for 4 h (CNT-3). In all these processes, the samples after acid treatment were filtered on a 0.22 μm Millipore polycarbonate membrane and rinsed with distilled water until the pH value of the filtrate became neutral. In process 4, the CNT-3 sample was further heat-treated in air at 400 °C for 45 min (CNT-4). The purpose of this additional heat treatment is to test if air oxidation at 400 °C can induce damage to the graphitic structure of SWCNTs.

The morphology and microstructure of the sample were studied using transmission electron microscopy (TEM) and high resolution TEM (HRTEM) (JEOL 2100F, accelerating voltage of 200 kV). To do this, the sample was dispersed in ethanol by means of a sonicator and scooped up with a holey amorphous carbon film. After different stages of heat treatment, the specimens were examined with X-ray diffraction (XRD). The X-ray diffractometer (Bruker D8 Advance, Bruker AXS) was operated at 40 KV and 40 mA. Nickel-filtered Cu Kα radiation was used in the incident beam. Raman spectroscopy (JOBLN-YVON T64000) was used to further characterize the structural integrity of the pristine and purified samples. Thermogravimetric analysis (TGA) (Pyrisdiamond TG/DTA) and near-infrared (NIR) spectroscopy were used to quantitatively characterize the pristine and purified SWCNTs. The NIR spectra were obtained on a Fourier transform NIR spectroscope (MPA, Bruker). For purity evaluation by NIR spectroscopy, 50 mg of a CNT sample was dispersed in 100 mL of dimethylformamide (DMF) solution by ultrasonication and mechanical stirring for 5 min. During this step, homogeneous CNT slurry was obtained. Then, a few drops of this slurry were further dissolved in 10 mL of DMF to obtain a faintly colored nonscattering dispersion after an additional 2 min of ultrasonication. Sonication was minimized to avoid damage to CNTs during sample preparation. The concentration of the dispersion was adjusted to be about 0.01 mg/mL to give the optimum signal-to-noise ratio for recording the spectra.

3. Results

Figure 1 shows the TEM images of the pristine sample. As can be seen in Figure 1a,b, entangled SWCNT bundles were mixed with a high density of metallic particles, as indicated by the numerous black dots. Except for these particles, multiwalled CNTs and carbon nanofibers were not observed. HRTEM (Figure 1c) revealed that the metallic nanoparticles were covered by carbon cages or shells with diameters ranging from 2 to 10 nm, and these cages consisted of several graphitic layers. These nanoparticles were presumably the result of the decomposition of ferrocene and ethanol. They were widely observed in the synthesis of SWCNTs by all previous methods.[8–11] The purpose of the present purification is to eliminate these particles.

(16) Monthioux, M.; Smith, B. W.; Claye, A.; Luzzi, D. E. *Carbon* **2001**, *39*, 1251–1253.
(17) Dujardin, E.; Ebbesen, T. W.; Krishnan, A.; Treacy, M. M. J. *Adv. Mater.* **1998**, *10*, 611–613.

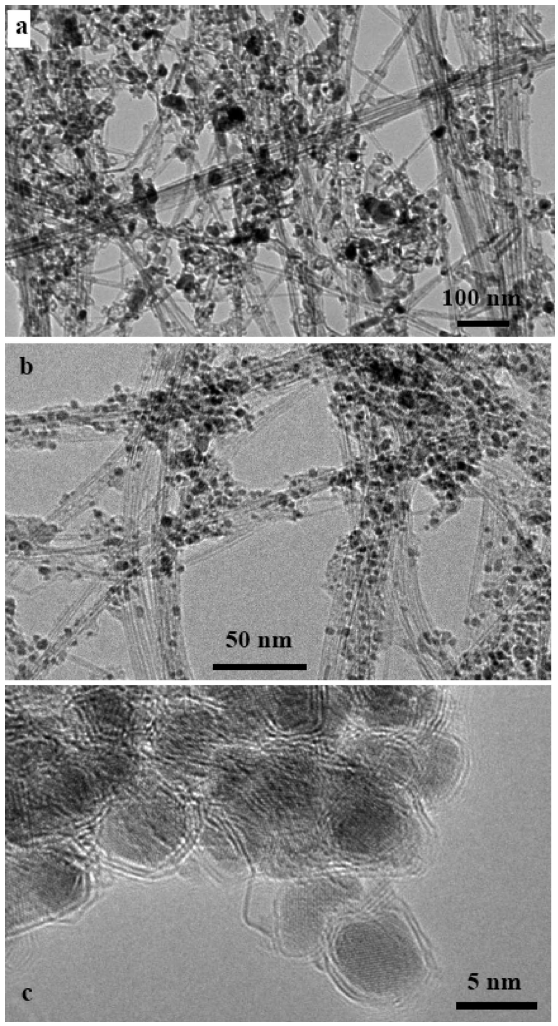

Figure 1. TEM images of the pristine sample (a, b) and iron particles embedded in graphitic shells (c).

The TEM images of the pristine samples after the three different purification processes are shown in Figure 2. It can be seen that after the purification by process 1 (air oxidation and HCl reflux), many metallic particles and hollow carbon cages remained (Figure 2a). After the purification by process 2 (air oxidation and HNO_3 reflux), even though the metallic particles were removed efficiently, empty carbon cages still persisted. Only after the purification by process 3 (high-temperature treatment and HCl reflux) could both the metallic particles and graphitic carbon cages be completely removed (Figure 2c,d). These observations suggest that high-temperature treatment assisted the purification and was critical to complete removal of impurities. The yield of material appears different after different purification processes, based on careful weighing. The yield is the lowest (35 wt %) for the case of purification by HNO_3 and 55 wt % for the case involving high-temperature treatment (Table 2). Thus, more material was lost during purification by HNO_3.

XRD analysis was used to understand the phase changes taking place during the processes of air oxidation and high-temperature treatment. Figure 3a shows the XRD pattern of the sample after air oxidation. There is no diffraction for graphite, indicating that there are very few or no MWCNTs in the sample. Only peaks which can be assigned to α-Fe_2O_3 are observed. Figure 3b shows the pattern for the sample after additional heat treatment in Ar at 800 °C. It can be

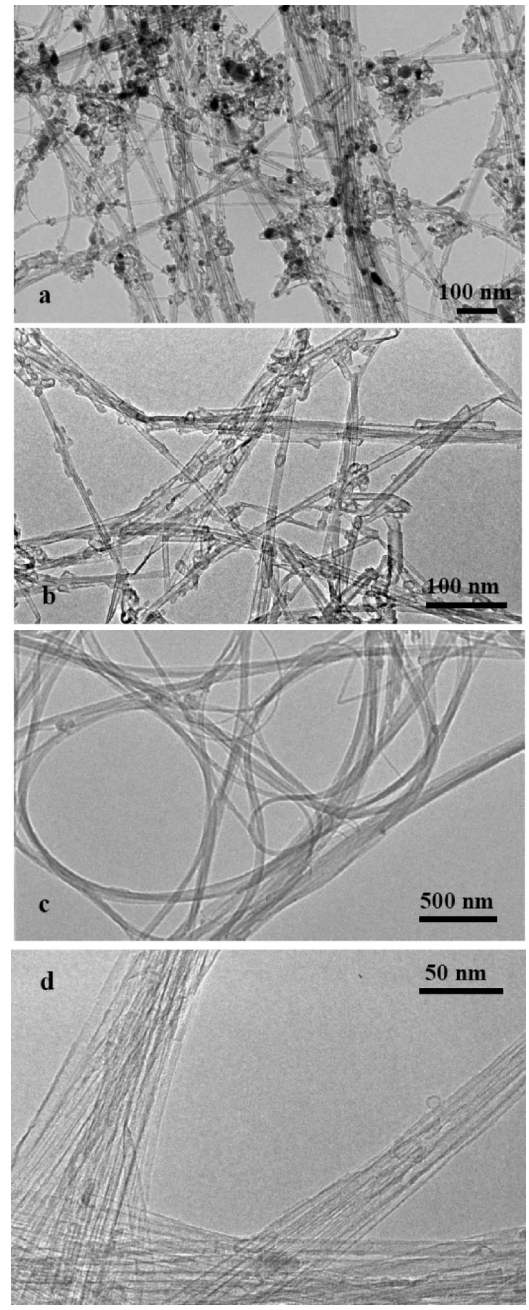

Figure 2. Typical TEM images of purified SWCNTs: (a) CNT-1. (b) CNT-2. (c, d) CNT-3.

Table 2. Analyses of the Pristine and Different Purified SWCNTs

sample	yield (wt %)[a]	Fe impurity (wt %)[b]	P_{NIR} (wt %)[c]	$P_{overall}$ (wt %)[d]	C impurity (wt %)[e]	I_G/I_D
CNT-0		27	46	33.6	39.4	7.3
CNT-1	65	12	62	54.6	33.4	11
CNT-2	35	2.5	28	27.3	70.2	3
CNT-3	55	3	96	93.1	3.9	19
CNT-4						18

[a] The yield of material by weighing after purification. [b] The Fe impurity contained in the pristine or purified sample, estimated from TGA results (Figure 5a). [c] The purity of SWCNTs estimated by using NIR spectroscopy. [d] The overall purity of SWCNTs in a sample when the residual Fe is taken into account. [e] The overall impurity of non-CNT carbons in a sample.

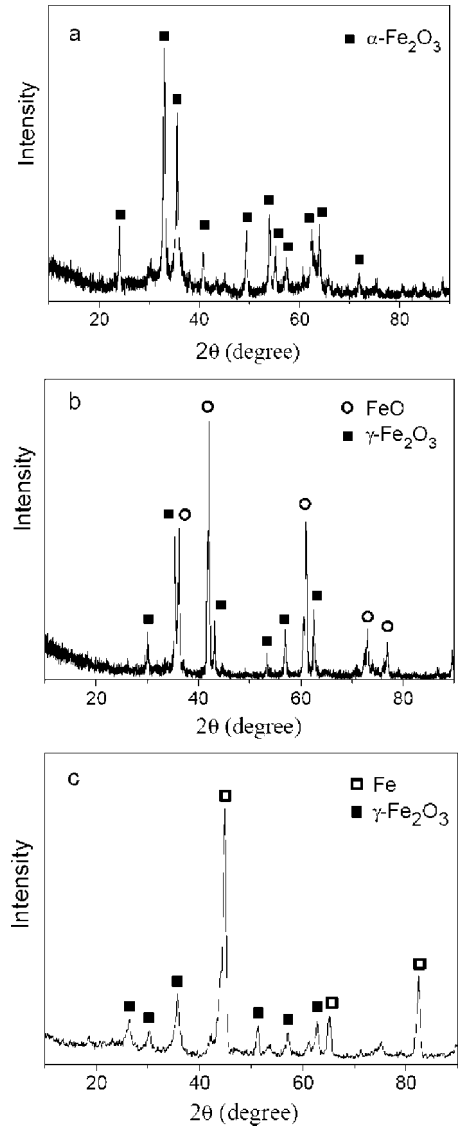

Figure 3. XRD patterns of the samples after heat treatments at different temperatures: (a) air oxidation at 400 °C, (b) air oxidation at 400 °C and heat treatment at 800 °C, and (c) air oxidation at 400 °C and heat treatment at 900 °C.

seen that clear FeO peaks could be distinguished in addition to those for γ-Fe_2O_3. Considering the presence of only α-Fe_2O_3 in the air-oxidized sample (Figure 3a), the appearance of FeO suggests partial reduction of α-Fe_2O_3 at 800 °C. Figure 3c illustrates the result of the sample after heat treatment in Ar at 900 °C. In this case, clear Fe peaks could be identified, although γ-Fe_2O_3 peaks are also found. Particularly, the FeO peaks seen for the sample heat-treated at 800 °C are no longer observed. Such observation suggests reduction of some α-Fe_2O_3 particles to Fe and transformation of the rest of the α-Fe_2O_3 particles to γ-Fe_2O_3 during heat treatment at 900 °C.

More detailed features of the present SWCNTs, such as purity, structural integrity, and diameter distribution, were examined by Raman spectroscopy, especially in the radial breathing mode (RBM), for samples of CNT-0 (pristine), CNT-1 (air oxidation and HCl reflux), CNT-2 (air oxidation and HNO_3 reflux), CNT-3 (high-temperature treatment and HCl reflux), and CNT-4 (high-temperature treatment, HCl reflux, and air oxidation). Figure 4a shows a low-frequency

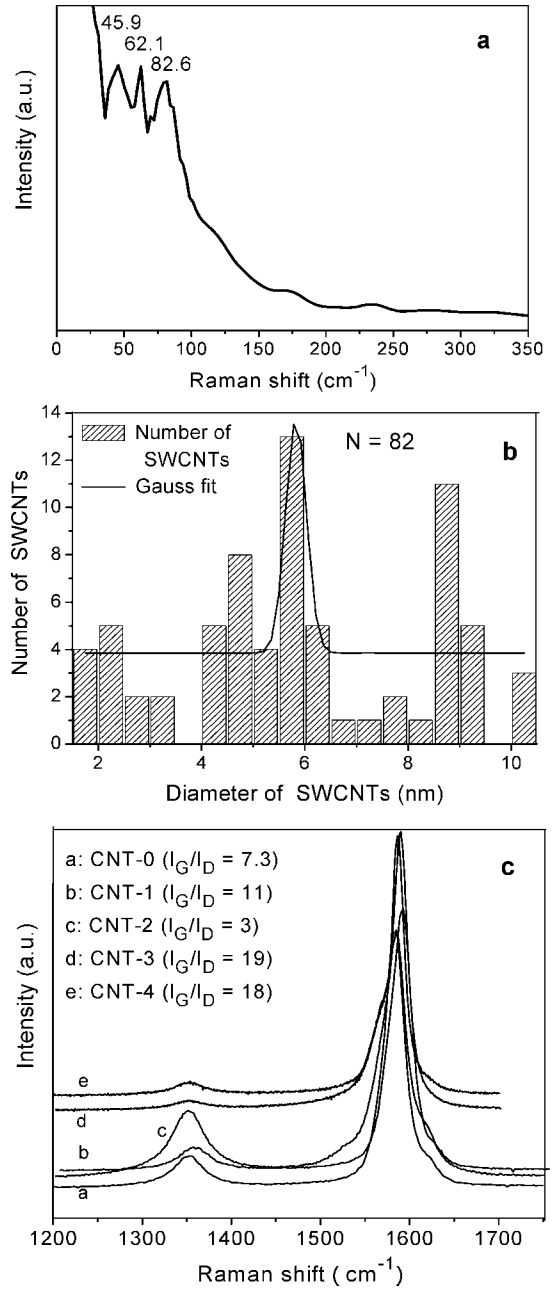

Figure 4. (a) Raman spectrum of CNT-3 at low frequency. (b) Histogram of diameter distribution of CNT-3. The solid line in the histogram is the Gaussian curve best fitting the distribution. (c) Raman spectra of pristine and purified samples at high frequency.

micro-Raman spectrum for CNT-3 shown in Figure 2c,d, measured with a laser excitation wavelength of 514.5 nm. The observed peaks correspond to the RBMs, the frequencies of which, ω_{RBM}, depend on the diameter of SWCNTs, d, by

$$\omega_{RBM} = A/d + B \quad (1)$$

where A and B are two constants. For typical SWCNTs, $A = 234$ cm^{-1} nm and $B = 10$ cm^{-1} have been found.[18,19] On the basis of eq 1 and the observed peaks at low frequencies, the diameters of the present SWCNTs are

(18) Milnera, M.; Kürti, J.; Hulman, M.; Kuzmany, H. *Phys. Rev. Lett.* **2000**, *84*, 1324–1329.
(19) Jorio, A.; Saito, R.; Hafner, J. H.; Lieber, C. M.; Hunter, M.; McClure, T.; Dresselhaus, G.; Dresselhaus, M. S. *Phys. Rev. Lett.* **2001**, *86*, 1118–1121.

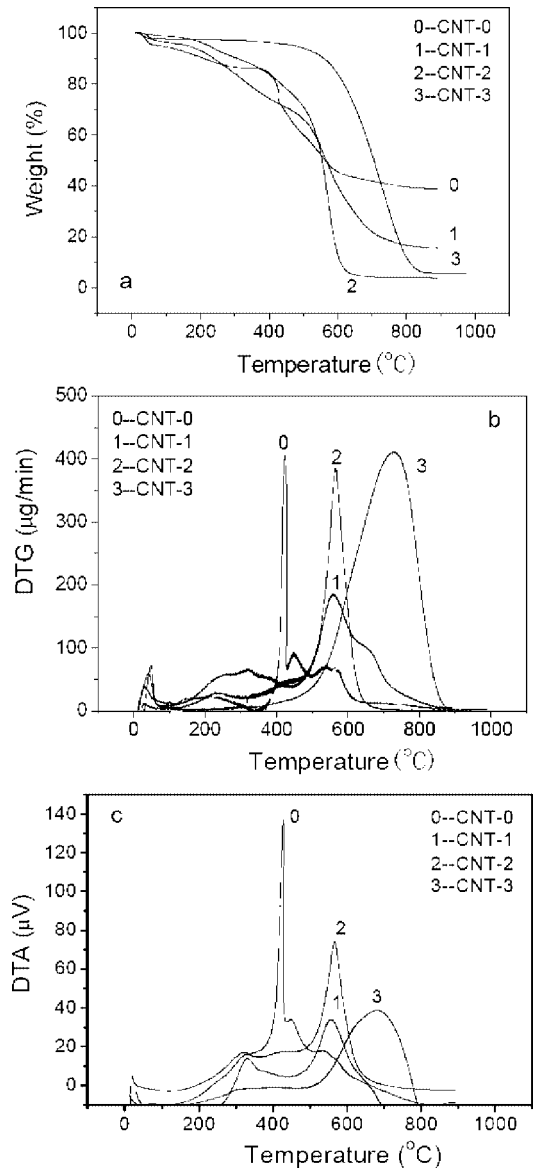

Figure 5. Thermal analysis curves of the pristine SWCNTs and the SWCNTs purified by different processes: (a) TG curves, (b) DTG curves, and (c) DTA curves.

calculated to be in the range of 3.2–7.0 nm. The diameter distribution of the present SWCNTs was also determined directly from HRTEM images. Statistic measurements show that while the diameters range from 1.75 to 10 nm, 78% of them lie in the range of 4–10 nm, with the Gaussian mean diameter being 5.8 nm (Figure 4b). This value is close to that obtained from eq 1.

The Raman spectra for the pristine and differently purified samples consist of two peaks at high frequencies (Figure 4c). The first peak appears at 1580 cm^{-1} as the so-called G peak related to E_{2g} graphite mode.[20–22] The strong intensity of this peak indicates good graphitization of CNTs. The second peak exists at around 1350 cm^{-1} as the D peak induced by a defect-related vibration mode.[20–22] The defects could include the minor amorphous carbon and graphitic carbon particles seen in the sample. The intensity ratio of the G and D peaks (I_G/I_D) is an indicator for estimating the purity of a SWCNT sample. As shown (Figure 4c, Table 2), the I_G/I_D ratio does not decrease after the purification by process 3. Actually, there is a great increase in this ratio as compared to that for CNT-0 (from 7.3 to 19). The ratios for these SWCNTs are all much higher than that for CNT-2 (I_G/I_D = 3). The I_G/I_D ratios for the samples of CNT-3 and CNT-4 are almost the same. This observation indicates that the graphitic structure of the present SWCNTs does not degrade during air oxidation at 400 °C.

The thermal analytic curves of all samples are presented in Figure 5. Inspection of the weight-loss behaviors (Figure 5a) shows that much more materials remained in the pristine sample than those in purified samples after air oxidation at temperatures up to 900 °C. This is an indication that there were much fewer catalytic particles left in the purified samples. Assuming that all carbonaceous materials have been oxidized and Fe particles oxidized to Fe_2O_3, the amount of Fe in each sample can be estimated. Such estimation reveals that the pristine sample CNT-0 contains 27 wt % Fe and CNT-2 and CNT-3 have about 3 wt % of residual Fe (Table 2).

As temperature increases, the sample of CNT-3 does not show weight loss until about 600 °C. Such an exclusive observation illustrates that this sample has a high purity of SWCNTs. Otherwise, weight loss, due to oxidation of carbon cages or/and amorphous carbon, could have commenced from a much lower temperature as observed for other samples. Additionally, the weight loss due to air oxidation appears to be complete at ~600 °C in the sample of CNT-2, but at 700 and 850 °C in the other two purified samples, suggesting destruction of the graphitic structure by HNO_3 treatment.

The temperatures at which the main thermal events take place during the whole oxidation process may be identified from the DTG/DTA curves (Figure 5b,c). While for the pristine sample (CNT-0), three events might occur at temperatures from 400 to 550 °C, the main thermal oxidation takes place at ~560 °C for the two acid-treated samples (CNT-1 and CNT-2) but at ~680 °C for the sample having undergone high-temperature treatment (CNT-3). This is an indication that the sample of CNT-3 is more oxidation-resistant than the other ones.

Recently, a method has been reported to quantitatively evaluate the purity of SWCNTs by using solution-phase NIR spectroscopy.[23,24] The content of SWCNTs in a sample could be evaluated by reference to a 100% pure SWCNT sample. An analytically pure SWCNT sample, though not yet available, is referred to that one originally prepared by arc discharge and then purified by a cross-flow filtration procedure.[23,24] SWCNTs give rise to a series of interband

(20) Dresselhaus, M. S.; Dresselhaus, G.; Jorio, A.; Souza Filho, A. G.; Saito, R. *Carbon* **2002**, *40*, 2043–2061.
(21) Souza Filho, A. G.; Jorio, A.; Samsonidze, G. G.; Dresselhaus, G.; Pimenta, M. A.; Dresselhaus, M. S.; Swan, A. K.; Ünlü, M. S.; Goldberg, B. B.; Saito, R. *Phys. Rev. B* **2003**, *67*, 035427–1–7.
(22) Grüneis, A.; Saito, R.; Kimura, T.; Cançado, L. G.; Pimenta, M. A.; Jorio, A.; Souza Filho, A. G.; Dresselhaus, M. S *Phys. Rev. B* **2002**, *65*, 1554051–7.
(23) Itkis, M. E.; Perea, D.; Niyogi, S.; Rickard, S.; Hamon, M.; Hu, H.; Zhao, B.; Haddon, R. C. *Nano Lett.* **2003**, *3*, 309–314.
(24) Itkis, M. E.; Perea, D.; Jung, R.; Niyogi, S.; Haddon, R. C. *J. Am. Chem. Soc.* **2005**, *127*, 3439–3448.

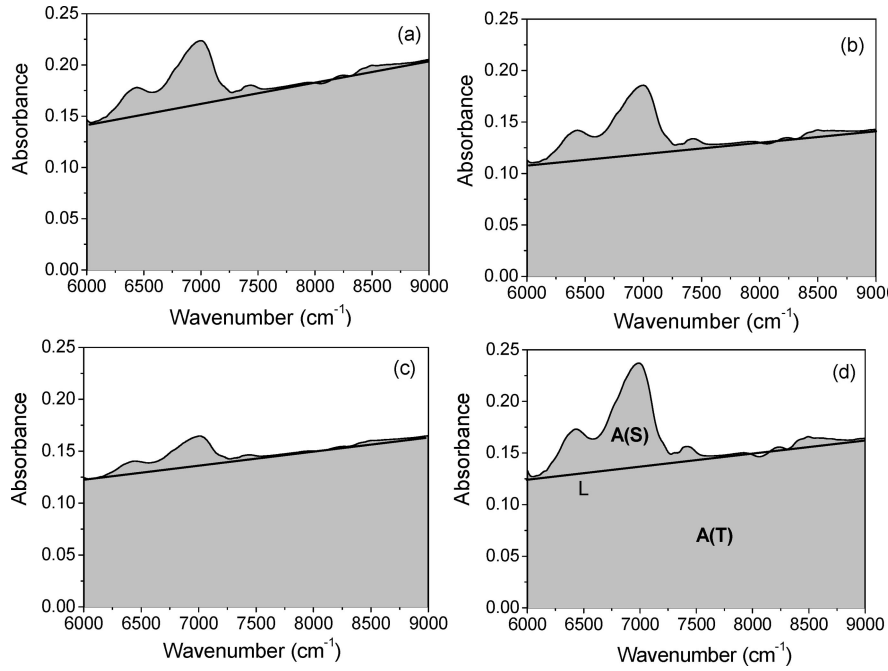

Figure 6. Absorption spectra of CNT-0 (a), CNT-1 (b), CNT-2 (c), and CNT-3 (d) samples in the range of the S_{22} interband transition. A(S) is the area above line L, and A(T) is the total area under the spectral curve.

electronic transitions. Since the transition at $S_{22} = 4\alpha\beta/d$, where α is the carbon−carbon bond length (nm), β is the transfer integral between pπ orbitals ($\beta = \sim 2.9$ eV), and d is the SWCNT diameter (nm), is much less affected by doping during chemical processing, it is usually used for purity evaluation.[23,24]

The S_{22} transitions of SWCNTs for the present samples are shown in Figure 6. The spectral cutoffs of 6000 cm^{-1} and 9000 cm^{-1} are chosen to capture the S_{22} bands. A strong upshift of S_{22} is observed relative to the reference sample with an S_{22} transition from 7750 to 11 750 cm^{-1}.[24,25] This is because the S_{22} absorption is known to have an energy that is an inverse function of the diameter[26,27] and the present SWCNTs have large diameters. Following the previous studies,[23,24] the ratio A(S)/A(T) is taken as the simplest possible metric of SWCNT purity, where A(S) is the area of the S_{22} interband transition after linear baseline subtraction and A(T) is the total area under the spectral curve (Figure 6d). This ratio is then normalized by dividing by 0.141, the value of A(S)/A(T) obtained for the reference sample. The SWCNT purity is then given by

$$P_{\mathrm{RBM}} = A(\mathrm{S})/0.141A(\mathrm{T}) \times 100\% \qquad (2)$$

Such determined P_{NIR} values for different purified samples are given in Table 2. The first observation is that the CNT-3 sample involving high-temperature treatment has a high purity of 96 wt %. This high purity approaches that for the reference sample (100 wt %). The second observation is that the CNT-2 sample involving HNO_3 has the lowest purity (even lower than that for the pristine sample). This observation indicates generation of carbon impurities during the purification process.

The purity estimation based on eq 2 includes SWCNTs as well as non-CNT carbons such as carbon nanocages and amorphous carbon. If the metal impurity, as determined from TGA analysis, is considered, the overall SWCNT purity (P_{overall}) and non-CNT carbon impurity in a sample can be calculated accordingly. Since the amount of residual Fe in the CNT-3 sample is low (3 wt %), the overall SWCNT purity is still very high in this sample (93 wt %) (Table 2).

4. Discussion

Complete removal of impurities, in particular, catalytic particles, encapsulating carbon cages, and amorphous carbon, is the first goal for purifying SWCNTs. The present study shows that only after the purification by process 3 (high-temperature treatment) could both the metallic particles and carbon cages be almost completely removed (Figure 2c). In contrast, the purification by either process 1 (HCl reflux) or process 2 (HNO_3 reflux) could not eliminate the metallic particles and carbon cages completely (Figure 2a,b). These observations suggest that the high-temperature treatment assisted the purification. Specifically, the amount of Fe particles could be lowered from the original 27 wt % to about 3 wt % (Table 2). Additionally, non-CNT carbons can be reduced to a very low level of 3.9 wt %, as revealed by the NIR spectroscopic approach (Table 2).

The present purification approach mainly relies on the following chemical reaction occurring at high temperature between Fe_2O_3 nanoparticles and the encapsulating graphitic carbon: $Fe_2O_3 + C \rightarrow Fe + CO_x$. It is the reduction of Fe_2O_3 by C that led to the consumption of C and thus the purification of SWCNTs, as shown by TEM in Figure 2c

(25) Kataura, H.; Kumazawa, Y.; Maniwa, Y.; Umezu, I.; Suzuki, S.; Ohtsuka, Y.; Achiba, Y. *Synth. Met.* **1999**, *103*, 2555–2558.
(26) Jost, O.; Gorbunov, A. A.; Pompe, W.; Pichler, T.; Friedlein, R.; Knupfer, M.; Reibold, M.; Bauer, H.-D.; Dunsch, L.; Golden, M. S.; Fink, J. *Appl. Phys. Lett.* **1999**, *75*, 2217–2219.
(27) Liu, X.; Pichler, T.; Knupfer, M.; Golden, M. S.; Fink, J.; Kataura, H.; Achiba, Y. *Phys. Rev. B* **2002**, *66*, 045411–045418.

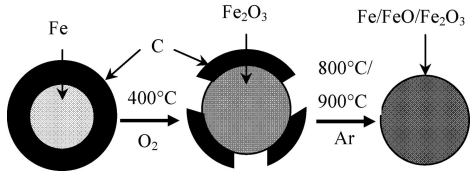

Figure 7. Schematic illustration of the removal of graphitic shells by air oxidation and high-temperature reaction.

and XRD in Figure 3b,c. The basic concept of the present purification is illustrated in Figure 7. First, as the sample is heated in air, Fe particles encapsulated in graphitic shells are oxidized to Fe_2O_3 (Figure 3a). When the sample is heated at 800 or 900 °C under Ar gas protection, the ferric oxide is reduced by the encapsulating carbon to FeO (800 °C, Figure 3b) or Fe (900 °C, Figure 3c). Since the previous encapsulating carbon (graphitic shells) has been completely oxidized, the remaining and exposed Fe or Fe oxide particles can be removed easily even by HCl.

The critical step of the present purification is the high-temperature treatment. Prior to this step, although Fe particles have been oxidized, and some encapsulating carbon might have been oxidized as well, the ferrous particles are still encapsulated by graphitic shells. Such shells, as shown in Figure 1c, are oxidation-resistant, protecting the enclosed particles from external chemical attack. After the first step of air oxidation, if the protecting shells had been oxidized, ferrous particles and carbon cages would not be observed after the purification by process 1 (HCl reflux only) or process 2 (HNO_3 reflux only). However, this is not the case, as shown in Figure 2a,b. It is the high-temperature treatment that removed graphitic shells. If graphitic shells still remained after this treatment, they could not be purified by HCl, as HCl is not a strong oxidative acid.

Complete removal of impurities with minimal destruction of the graphitic structure of SWCNTs is the second goal. Previous gas-phase or liquid-phase chemical oxidation is not able to easily remove the graphitic particles and shells, since these particles are resistant to oxidation. In order to remove them and obtain high-purity SWCNTs, severe oxidation conditions, such as a high concentration of HNO_3 acid or a long reaction time, must be imposed, as in recent studies.[28,29] However, the severe conditions invariably introduce defects into SWCNTs.

The introduction of defects and damage of the graphitic structure of SWCNTs by HNO_3 was also observed in the present study. After air oxidation and refluxing in HNO_3, the CNT-2 sample has the lowest purity of SWCNTs (P_{NIR} = 28 wt %) (even lower than that for the pristine sample, P_{NIR} = 46 wt %). This decrease in SWCNT purity indicates that purification with HNO_3 destroys SWCNTs, as suggested before,[30] and produces carbonaceous impurities in the sample. In contrast, with the purification involving high-temperature treatment, the SWCNT purity of P_{NIR} (=96 wt %) is two times higher than that for the pristine sample (P_{NIR} = 46 wt %) and actually close to that for the reference sample assumed to have P_{NIR} = 100 wt %. All these data from NIR spectroscopy suggest that the purification involving high-temperature treatment is advantageous over that by HNO_3 in maintaining the graphitic structure of SWCNTs, although the Fe content can be reduced to the same low level of ~3 wt % by these two processes.

The same conclusion can be drawn from Raman spectroscopic and TGA results. The observations include a smaller ratio of I_G/I_D (Figure 4) and a lower oxidation temperature for the sample purified by process 2 than those for other samples (Figure 5). In contrast, the sample purified by process 3 has a much larger ratio of I_G/I_D (Figure 4) and a higher oxidation temperature (Figure 5) than other samples. This observation suggests that the graphitic structure of SWCNTs might not be damaged or is little damaged by the purification of process 3. The reason may be that the oxidation at 400 °C in the first step only induced oxidation of Fe particles but not SWCNTs. This is confirmed by the observed high I_G/I_D ratio for the sample of CNT-4 (Figure 4). If the air oxidation induced structural damage, the ratio of this sample could be expected to decrease. As a matter of fact, the TG curve (Figure 5a) shows that for the pristine sample significant material loss involving oxidation of SWCNTs occurs at temperatures higher than 400 °C. In addition, the high-temperature treatment induced the reaction of ferrous particles with encapsulating graphitic shells but not SWCNTs. If the ferrous particles reacted with SWCNTs, fragmentation of SWCNTs would be observed. But Figure 2c shows that this is not the case. Therefore, none of the three steps in process 3 (air oxidation at 400 °C, Ar protected reaction at high temperature, and reflux in HCl) is destructive to the graphitic structure of SWCNTs, and the purification may be considered as nondestructive.

Complete removal of impurities with minimal loss of SWCNTs is the third goal. In order to remove the catalytic and graphite particles and obtain high-purity SWCNTs, severe oxidation conditions must be imposed in previous gas-phase or liquid-phase chemical methods. However, the severe conditions inevitably introduce not only defects but loss of SWCNTs as well. For example, the graphitic shells in the present pristine sample may be oxidized by raising the temperature of air oxidation from 400 °C to a higher temperature. As a result, more or even all graphitic shells may be oxidized, leaving bare iron oxide particles. However, at temperatures higher than 400 °C, all samples shown in Figure 5, including the pristine and purified ones, suffer from significant material loss. Such material loss includes not only the graphitic shells but also SWCNTs. In the present study, the loss of SWCNTs was minimized by air oxidation at a temperature not high enough for inducing oxidation of SWCNTs. The observed high I_G/I_D ratios for the samples of CNT-3 and CNT-4 (Figure 4) show that the air-oxidation process causes little damage to SWCNTs. Since lattice damage and material loss of SWCNTs generally occur at the same time, the observed higher I_G/I_D ratio (Figure 4),

(28) Hu, H.; Zhao, B.; Itkis, M. E.; Haddon, R. C. *J. Phys. Chem. B* **2003**, *107*, 13838–13842.
(29) Park, J. J.; Banerjee, S.; Hemraj-Benny, T.; Wong, S. S. *J. Mater. Chem.* **2006**, *16*, 141–154.
(30) Sen, R.; Rickard, S. M.; Itkis, M. E.; Haddon, R. C. *Chem. Mater.* **2003**, *15*, 4273–4279.

higher thermal stability (Figure 5), and higher P_{NIR} value suggest a low material loss and nondestruction in the present purification involving high-temperature treatment.

5. Conclusions

A new method is demonstrated for purification of SWCNT samples. This involves transformation of catalytic iron particles to iron oxide at low temperature, subsequent removal of the graphitic shells by reaction with the encapsulated iron oxide at high temperature, and final elimination of iron oxide particles by HCl. Experimental results show that catalytic particles and encapsulating graphitic shells can be efficiently removed. More importantly, the highly efficient purification induces little damage to the graphitic structure of SWCNTs as evidenced by TEM, TGA, Raman, and NIR spectroscopic studies. The present method may be applied for highly efficient and nondestructive purification of CNT materials of any origin to be used in wide areas.

Acknowledgment. J.N.W. appreciates the Outstanding Youth Fund from The National Natural Science Foundation of China and the National 863 Project of 2007AA05Z128 from the Ministry of Science and Technology of China.

CM8001699